PERGAMON

International Journal of Heat and Mass Transfer 44 (2001) 2589–2599

International Journal of HEAT and MASS TRANSFER

www.elsevier.com/locate/ijhmt

Effects of heater size and orientation on pool boiling heat transfer from microporous coated surfaces

K.N. Rainey [a], S.M. You [b,*]

[a] *Department of Mechanical and Aerospace Engineering, The University of Texas at Arlington, PO Box 19023, Arlington, TX 76019-0023, USA*

[b] *School of Mechanical and Aerospace Engineering, Seoul National University, San 56-1, Shinrim-Dong, Kwanak-Gu, Seoul 151-742, South Korea*

Received 6 June 2000; received in revised form 11 October 2000

Abstract

The present research is an experimental study of pool boiling behavior using flat, microporous-enhanced square heater surfaces immersed in saturated FC-72. Flush-mounted 2 cm × 2 cm and 5 cm × 5 cm copper surfaces were tested and compared to a 1 cm × 1 cm copper surface that was previously investigated. Heater surface orientation and size effects on pool boiling performance were investigated under increasing and decreasing heat-flux conditions for two different surface microgeometries: plain and microporous coated. Results of the plain surface testing showed that the nucleate boiling performance is dependent on heater orientation. The nucleate boiling curves of the microporous coated surfaces were found to collapse to one curve showing insensitivity to heater orientation. The effects of heater size and orientation angle on CHF were found to be significant for both the plain and microporous coated surfaces.

1. Introduction

Among the first researchers to study the effect of orientation on the nucleate boiling heat transfer was Storr [2], who observed that the heat transfer rate for a given wall superheat increased when rotating his heating surface from horizontal to vertical. Marcus and Dropkin [3] and Githinji and Sabersky [4] have also found that the heat transfer coefficient increases from an inclination angle of 0° (horizontal, upward facing) to 90°. Marcus and Dropkin have described the phenomenon as the result of increased agitation of the superheated boundary region due to the increased path length of the departing bubbles along the surface. Further research indicated that the heat transfer coefficient continues to increase up to an angle between 150° and 175° and then decreases drastically as the angle approaches 180° [5–7]. Chang and You [8], using a small copper surface in FC-72 saw similar results between 0° and 90°, however, they found that the heat transfer coefficient decreased for angles greater than 90°.

Marcus and Dropkin have additionally hypothesized that the nucleate boiling heat transfer coefficient would become insensitive to inclination angle above a certain heat flux. Nishikawa et al. [5] have confirmed the existence of this transition heat flux. Lienhard [9] has related Nishikawa et al.'s observed transition point to the transition from the isolated bubble regime to the continuous vapor column regime as described by Zuber [10] and Moissis and Berenson [11]. Similar trends were reported by Beduz et al. [6]. Beduz et al. have also found that the heat transfer coefficient was independent of inclination angle for their enhanced surface. Angular independence of the nucleate boiling heat transfer coefficient for other enhanced surfaces has also been shown by Jung et al. [12] and Chang and You [8].

One of the first researchers to study the effects of inclination angle on q''_{CHF} was Githinji and Sabersky [4]. Using a relatively long and thin heating surface (102 mm × 3.2 mm) in water, they found that the q''_{CHF} increased from 0° to 90° and then decreased drastically from 90° to 180°. Using a smaller surface (9.9-mm

* Corresponding author. Tel.: 02-880-7110; fax: 02-883-0179.
E-mail address: smyon@snu.ac.kr (S.M. You).

0017-9310/01/$ - see front matter
PII: S0017-9310(00)00318-5

Nomenclature

g	acceleration due to gravity (m/s^2)
h_{lv}	latent heat of vaporization (J/kg)
L	surface side length (m)
L'	dimensionless surface length $L' = L[g(\rho_l - \rho_v)/\sigma]^{0.5}$
q''	heat flux (W/m^2)

Greek symbols

β	liquid–surface contact angle (°)
ΔT_{sat}	wall superheat (K)
θ	surface inclination angle from horizontal upward position (°)
ρ	density (kg/m^3)
σ	surface tension (N/m)

Subscripts

0°	$\theta = 0°$ (horizontal, upward facing)
CHF	critical heat flux
l	saturated liquid
tr	transition point from isolated bubbles to continuous vapor columns
v	saturated vapor
Z	CHF prediction of Zuber [1]

diameter) in liquid helium, Lyon [13] has observed that q''_{CHF} continually decreases from 0° to 180°. This last trend has been the dominant trend seen in the literature. Among the first to correlate the effect of orientation on q''_{CHF} was Vishnev [14]. His correlation was developed for cryogenic fluids based on the helium data of other researchers. Later, El-Genk and Guo [7], using numerous sources of data, have developed separate correlations for water, nitrogen, and helium. More recently, Chang and You [8] have correlated their FC-72 data and checked it against both cryogenic and non-cryogenic fluids from many sources. Howard and Mudawar [15] have developed a CHF model for the near-vertical pool-boiling situation based on their observations in FC-72.

The effects of size on pool boiling heat transfer have been studied previously. At an inclination angle of 0° (horizontal, upward facing), Gogonin and Kutateladze [16] did not see any observable change in q''_{CHF} when they varied the width of their heating surface. Ishigai et al. [17] have found that q''_{CHF} decreased with increasing heater size at an inclination of 180°. Similar trends were reported by Gogonin and Kutateladze [16] and Granovskii et al. [18]. Using 0° oriented flat surfaces with sidewalls, Lienhard, et al. [19] have showed both analytically and experimentally that, in general, q''_{CHF} would decrease with increasing heater size up to a point and then become relatively constant. They related this behavior to the number of "vapor jets" that could be supported by the surface area. Similarly, Saylor et al. [20] have found that q''_{CHF} was relatively constant for large surfaces and increased for decreasing heater size past a certain transition point. Park and Bergles [21] have observed that the nucleate boiling heat transfer coefficient was insensitive to heater size. Additionally, Park and Bergles have found that q''_{CHF} was affected by changes in both height and width in similar trends as those later observed by Saylor et al. for 0° oriented surfaces.

The objective of the present research is to understand the combined effects of heater surface orientation and size on pool boiling behavior of flat, square heater surfaces immersed in saturated FC-72. Two surface conditions were considered: plain and microporous coated. To study the effect of orientation, six different heater orientation angles (0°, 45°, 90°, 135°, 160°, and 180°) were used. To study the effect of heater size, two relatively large surfaces, 4-cm^2 (2 cm × 2 cm) and 25-cm^2 (5 cm × 5 cm), were tested. The results were then compared to the results of Chang and You [8] who studied a 1-cm^2 (1 cm × 1 cm) heater surface. For the plain surface tests, two different heat flux conditions, increasing and decreasing, were also considered.

2. Experimental apparatus and procedure

2.1. Test facility

The 4-cm^2 heater was tested in the same test facility as used for the 1-cm^2 heater of Chang and You [8] and is described in detail in their paper. The pool boiling test facility used for the 25-cm^2 heater is shown in Fig. 1. The test fluid, FC-72, is a highly wetting dielectric perfluorocarbon produced by the 3M Industrial Chemical Products Division. FC-72 has been determined to be a good candidate fluid for immersion cooling applications because it is chemically stable/inert, dielectric, and has a relatively low boiling point ($T_{sat} = 56$°C at 1 atm). The test liquid was contained within a stainless steel pressure vessel, 406-mm high and 154-mm in diameter, which was heated by three band heaters located on the sides and bottom of the chamber. A cartridge heater was located in the bottom of the chamber to provide additional heating during degassing and in between individual tests. The test vessel was insulated with a 15-mm thick foam. An external, water-cooled condenser was used throughout the testing to prevent loss of test liquid. An internal, water-cooled condenser was utilized for the 25-cm^2 heater when the heater power exceeded 12 W/cm^2 to prevent excessive liquid holdup in the external con-

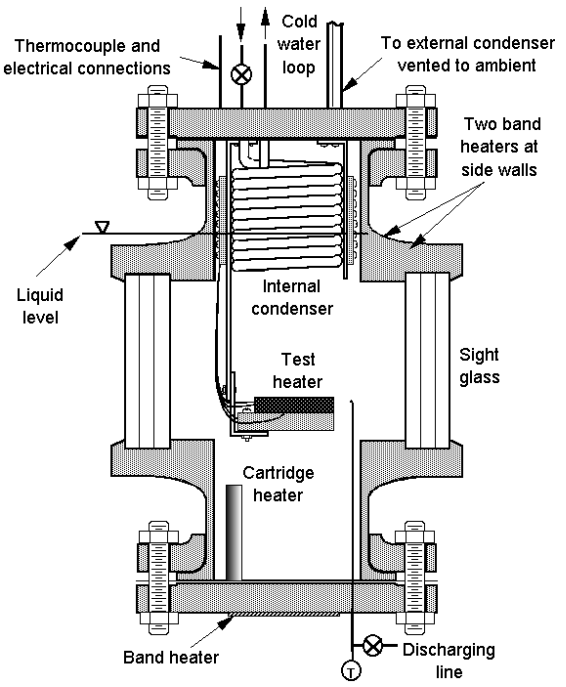

Fig. 1. Test section schematic.

denser's vapor/liquid line. A copper–constantan thermocouple was placed within the test vessel to measure the bulk liquid temperature. Atmospheric pressure was maintained by venting the vessel to ambient. The test heater assembly was mounted to a stainless steel support bar, which enabled rotation of the surface to any desired inclination angle, and immersed in the test liquid. The test liquid surface was maintained at approximately 150 mm above the test heater surface.

A DC power supply was connected in series with a shunt resistor and the test heater. The shunt resistor, rated at 100 mV and 10 A, was used to determine the current in the electric circuit. The measured voltage drop across the test heater was used to calculate the heat flux applied to the test heater.

The present test heater design is the same as that used by Chang and You [8]. Fig. 2 shows the 4-cm^2 test heater assembly. For the 4-cm^2 heater, a serpentine winding of Ni–Cr wire (0.144-mm diameter) was attached to a Teflon substrate (11-mm thick) using Omegabond 200 high-temperature epoxy (thermal conductivity of $\approx$1.4 W/m K). The winding was soldered to copper strips and provided a total heating element resistance of $\approx$30 Ω. A 20 mm $\times$ 20 mm $\times$ 3.2 mm thick block of copper was bonded on top of the heating element using the same epoxy. Two layers of epoxy assured electrical insulation. To provide surface temperature measurements, two copper–constantan thermocouples were inserted and

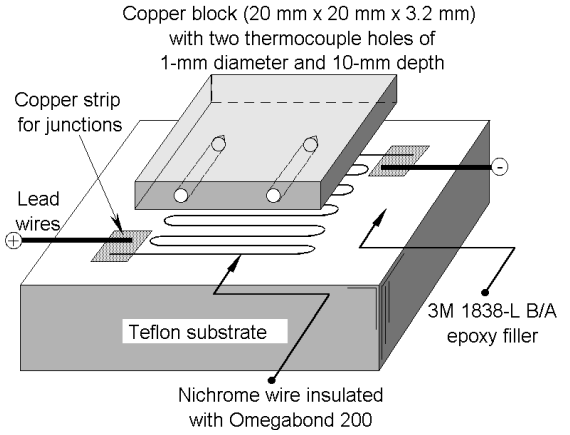

Fig. 2. 4-cm^2 test heater assembly.

soldered into two holes (1-mm diameter and 10-mm depth) drilled in the center of the copper block thickness. The thermocouple holes were placed 5 mm from the edges and 10 mm apart as indicated in Fig. 2. The completed test heater was then mounted in a Lexan frame and surrounded by a two-part 3M epoxy (1832L-B/A, thermal conductivity of $\approx$ 0.067 W/m K) to generate a flush-mounted heating surface. The copper surface of the heater was polished using Brasso metal polish. The 25-cm^2 heater was constructed in an identical manner except that the two embedded thermocouples were placed 12.5 mm deep, 12.5 mm from the edges, and at opposite corners.

For the microporous coated heater tests, the coating used is the DOM coating. The coating is a surface treatment technique used to increase vapor/gas entrapment volume and active nucleation site density by forming a porous structure with cavities much smaller than conventional metallic porous coatings. The DOM coating was named from the initial letters of its three components: **D**iamond/**O**megabond 101/**M**ethyl-Ethyl-Ketone (MEK). The mixture of the three components was drip-coated over the 4-cm^2 plain surface using a paintbrush and spray-coated over the 25-cm^2 plain surface using an airbrush. After the carrier (MEK) evaporated, the resulting coated layer consisted of dielectric, microporous structures with diamond particles (8–12 μm) and a binder (Omegabond 101) having a thickness of $\approx$50 μm. Detailed descriptions of the coating are provided by O'Connor et al. [22] and Chang and You [23,24].

2.2. Test procedure

The test chamber was heated to the test liquid's saturation temperature using the three band heaters and the cartridge heater. Once at its saturation temperature,

the test liquid was boiled vigorously for two hours to remove the dissolved gases before testing. Boiling curves were then generated at orientation angles of 0°, 45°, 90°, 135°, 160°, and 180° for each surface tested. A single test was performed for each angle. There was a two-hour delay between tests to allow the heater surface and test section to return to steady state. After each of the six different angular positions was completed, the 0°-orientation pool boiling curve was reproduced for each surface tested. Identical pool boiling curves at 0° for each surface assured the consistency and repeatability of the data.

Heat flux was controlled by voltage input. After each voltage change (heat-flux increment or decrement), a 15-s delay was imposed before initiating the data acquisition. After the delay, the computer repeatedly collected and averaged 125 base surface temperature measurements over 15 s until the temperature difference between two consecutive averaged temperature measurements for all thermocouples was less than 0.2 K. The test section at this point was assumed to be at steady state. After reaching steady state, heater surface and bulk fluid temperatures were measured and the heat flux was calculated. For heat-flux values greater than ≈80% of q''_{CHF}, instantaneous surface temperature was monitored for 45 s after each increment to prevent heater burnout. Each instantaneous surface temperature measurement was compared with the previous increment's average surface temperature. If a temperature difference larger than 20 K was detected, q''_{CHF} was assumed and the power shut off. The q''_{CHF} value was computed as the steady-state heat-flux value just prior to power supply shutdown plus half of the increment. For the tests under decreasing heat-flux conditions, the initial heat-flux point was approximately 80% of q''_{CHF}.

3. Experimental uncertainty

Uncertainty in the heat-flux measurement was estimated based on the values of Chang and You [8], whose heater had the same design as the present one. Chang and You estimated the uncertainty, including substrate conduction and heat flux measurement uncertainty, to be smaller than 5% for a heat flux of 15 W/cm^2. The uncertainty estimates of the present heaters can be estimated to be smaller than that of Chang and You for the larger surface areas (4.0 and 25.0 vs. 1.0 cm^2) due to lower substrate conduction heat loss. Temperature measurement uncertainty was estimated considering thermocouple calibration error, temperature correction for the embedded thermocouples, and thermocouple resolution error. The uncertainty in temperature measurement was ±0.4 K. In addition, the uncertainty in orientation angle is estimated at ±0.5°.

4. Results and discussion

The present study is to understand the combined effects of surface size and orientation on nucleate boiling and CHF for microporous coated surfaces. The experimental data used in this study come from both the present and previously published data. The data for the 1-cm^2 surface at orientation angles of 0° (horizontal, upward facing), 45°, 90°, 135°, and 180° come from Chang and You [8] while the data for the 1-cm^2 heater at 160°, the 4-cm^2 heater data, and 25-cm^2 heater data comprise the present work. The methods of construction, surface preparation, and testing for Chang and You's previous analysis are the same with the present work. Therefore, a direct integration of Chang and You's data with the present study is possible.

5. Pool boiling tests of reference surfaces ($\theta = 0°$)

Fig. 3 illustrates the saturated plain (polished) surface pool boiling test results at $\theta = 0°$ for the three different size heaters. The natural convection data of the present heaters show that the 4- and 25-cm^2 surfaces have about 30% and 35% lower heat transfer coefficients, respectively, than the 1-cm^2 surface. The incipient superheat values are seen to decrease with increasing size as well. Incipient superheat values range from 20 to 35 K for the 4-cm^2 surface and 16 to 17 K for the 25-cm^2 surface which are lower than the range of 25–40 K reported by Chang and You [8] for their 1-cm^2 surface. This decreasing trend can be primarily attributed to surface irregularities caused by slight differences in sur-

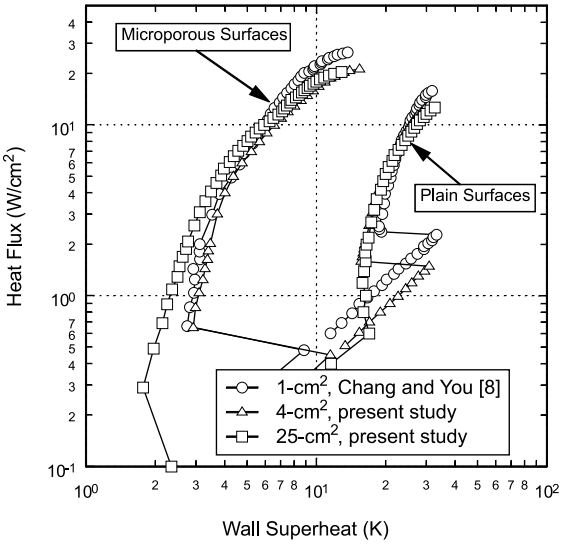

Fig. 3. Reference surfaces' pool boiling data ($\theta = 0°$, increasing heat flux).

face preparation. The larger heaters are more likely to have not been polished as consistently as the smaller heaters allowing for the presence of larger surface cavities, which would produce earlier incipience. The q''_{CHF} values ranged between 12.6–13.1 W/cm^2 for the 4-cm^2 surface and 12.9–13.2 W/cm^2 for the 25-cm^2 surface which are slightly lower than the range of 13.2–16.0 W/cm^2 for the 1-cm^2 surface reported by Chang and You [8]. In comparison, Zuber's [1] correlation given by:

$$q''_{CHF,Z} = \frac{\pi}{24} h_{lv} \rho_v^{1/2} [g\sigma(\rho_l - \rho_v)]^{1/4} \quad (1)$$

predicts $q''_{CHF,Z} = 15.1$ W/cm^2 for saturated FC-72.

Fig. 3 also illustrates the saturated microporous coated surface pool boiling test results at $\theta = 0°$ for the three different size surfaces. All the microporous coated surfaces showed incipient superheats of less than 12 K, which is significantly lower than the plain surface values. Upon incipience, the microporous coated surfaces produced nucleate boiling over their entire surface area, generating discrete tiny bubbles less than 0.2 mm in diameter. As shown in Fig. 3, the reference-surface natural convection regimes of the plain surfaces were replaced almost entirely by the nucleate boiling regime of the microporous coated surfaces. Throughout the nucleate boiling regime, the microporous coated surfaces consistently augmented heat transfer coefficients by more than 300% when compared to those of the plain surfaces. This enhancement is the result of the dramatically increased active nucleation site density caused by the surface microstructures provided by the microporous coating. The present 4-cm^2 microporous coated surface exhibited a consistent q''_{CHF} value of 21.5 W/cm^2 while the 25-cm^2 surface showed q''_{CHF} values ranging from 20.6 to 21.7 W/cm^2. These values are slightly lower than the q''_{CHF} value of 26.8 W/cm^2 that Chang and You [8] reported for their 1-cm^2 surface.

For both the plain and microporous surfaces, the 1-cm^2 heaters showed significantly higher CHF values than the 4- and 25-cm^2 heaters. Fig. 4 illustrates the effect of surface size on q''_{CHF} at 0°. In Fig. 4, the present data are plotted with the data of Saylor et al. [20]. The data are normalized with respect to Zuber's CHF, Eq. (1), and plotted versus a dimensionless length scale, L'. As can be seen from Fig. 4, the present data follow the same trend as Saylor et al.'s data although shifted upward. The q''_{CHF} values are asymptotic for large surfaces and then suddenly increase with decreasing surface size below a certain "transition"point. Bar-Cohen and McNeil [25] determined that the transition point was $L'_{trans} \approx 20$ (which is equivalent to a 1.5 cm × 1.5 cm surface for the present study). The present data appear to support Bar-Cohen and McNeil's estimate for L'_{trans}. Although the asymptotic q''_{CHF} values are much higher, the microporous coated surfaces appear to have the same transition L' value (≈20) as the plain surfaces.

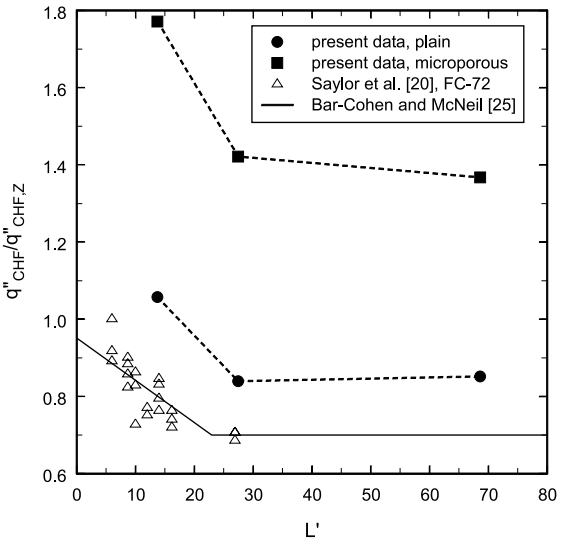

Fig. 4. Effect of heater size on CHF ($\theta = 0°$).

The above observations at an inclination angle 0° can be explained in terms of fluid re-wetting. As the heat flux increases, the amount and time of vapor covering the surfaces increase, which, in turn, increases the re-wetting resistance to the cooler bulk liquid approaching the heater surface. For small surfaces, a significant portion of the re-wetting fluid is supplied from the sides rather than from above, as in an infinite flat plate situation. The re-wetting resistance should be a function of flow path length parallel to the heater surface. Compared to Chang and You's [8] smaller 1-cm^2 surface, the larger 4- and 25-cm^2 surfaces have longer fluid paths to reach the center portion of the heater surface and hence relatively smaller entrance flow areas from the sides compared to their heater surface areas. Because of this increased re-wetting resistance, the larger surfaces experienced higher wall superheats near q''_{CHF} and thus lower q''_{CHF} values.

In Fig. 5, bubble patterns at q''_{CHF} are compared for the 0° inclined plain and microporous coated surfaces of the 4-cm^2 heater. For the plain surface case in Fig. 4(a), a film-boiling pattern was observed on the heater surface. A five-bubble pattern and a four-bubble pattern alternately formed consistently from the heater surface. Lienhard et al. [19] have performed an analysis for finite horizontal flat plates with vertical sidewalls to approximate an infinite flat plate based on the most susceptible Taylor wavelength (≈8 mm for saturated FC-72 at atmospheric pressure) and the number of vapor jets that can be supported by the surface area. The bubble pattern observed in Fig. 4(a) is consistent with Lienhard et al.'s theoretical calculations of vapor jet patterns at q''_{CHF}. However, for the microporous coated surface in Fig. 4(b), random bubble clusters were observed instead of the consistent alternation of a four- and five-bubble

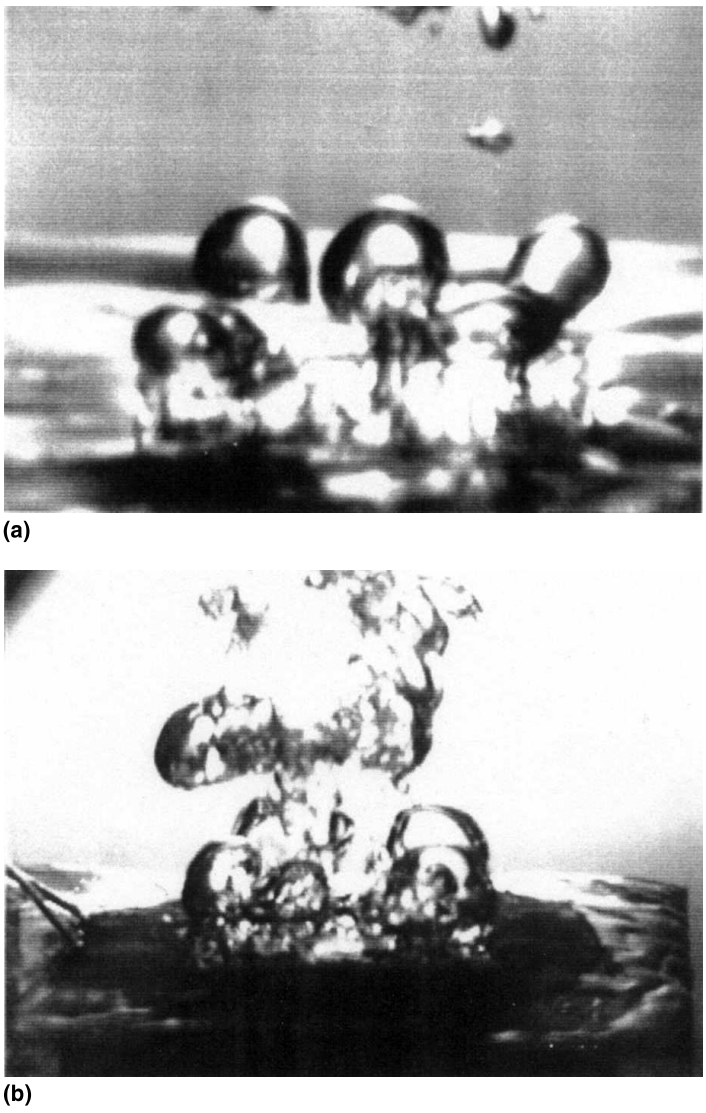

Fig. 5. Photographs of CHF phenomenon for 4-cm^2 heater ($\theta = 0°$): (a) plain surface; (b) microporous surface.

pattern. Because the film-boiling pattern was disturbed by the small bubbles from the microporous coated surfaces as shown in the figure, the film-boiling pattern could not be clearly observed.

5.1. Heater orientation effect for plain surfaces

The test results of orientation effect for the plain surfaces under increasing heat-flux conditions are presented in Figs. 6–8. In Fig. 6, the 160° test point has been added to Chang and You's [8] data to provide a complete test matrix for comparison. For clarity, only the nucleate boiling regions are presented in Figs. 6–8. The most obvious trend in the nucleate boiling behavior with respect to orientation is the dramatic decrease in heat transfer performance, which occurs when increasing the inclination angle from 90° to 180°. For the downward-facing inclinations ($\theta > 90°$), the departing bubbles tended to flatten against the surface and merge with neighboring bubbles. The bubbles also exhibited a noticeably reduced rise velocity. This flattening and reduced rise velocity of the bubbles cause the residence time of the vapor bubbles, as well as the vapor quality, to increase near the heater surface, which increases the resistance to heat transfer. At an inclination angle of 180°, the vapor residence time near the surface increased enough to allow the formation of large, slow-moving vapor bubbles which covered a large portion of the

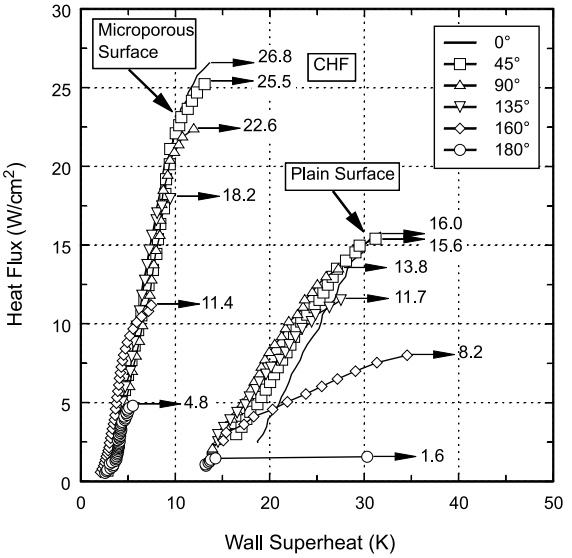

Fig. 6. Effects of inclination angle for 1-cm^2 surface (increasing heat flux, [8]).

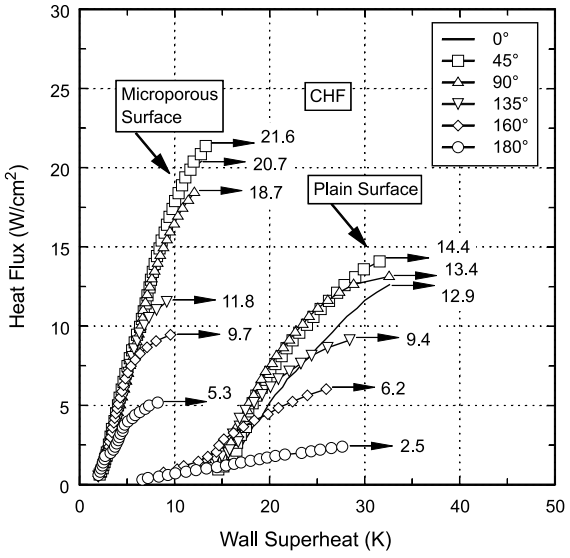

Fig. 8. Effects of inclination angle for 25-cm^2 surface (increasing heat flux).

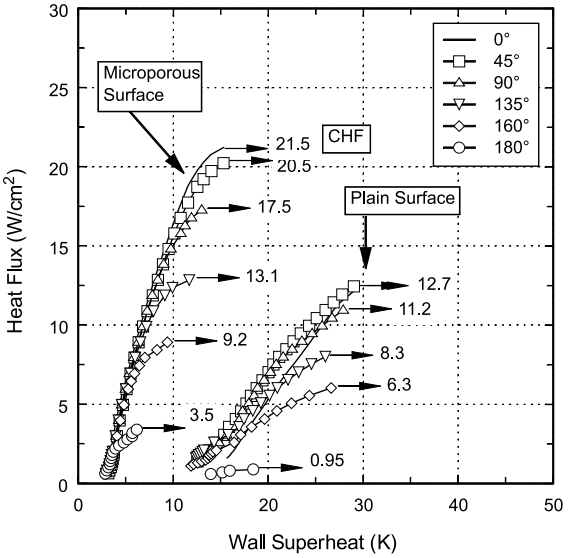

Fig. 7. Effects of inclination angle for 4-cm^2 surface (increasing heat flux).

heated surface. The increased thermal resistance due to these large vapor bubbles produced very low q''_{CHF} values: 1.6, 0.95 and 2.5 W/cm^2 for the 1-, 4- and 25-cm^2 surfaces, respectively. The boiling crisis mechanism in this case would be better described as a combined hydrodynamic/dry-out CHF.

Chang and You [8] have observed an increase in the heat transfer performance in the lower nucleate boiling heat-flux region from $\theta = 0°$ to 45° of their 1-cm^2 surface as shown in Fig. 6. Chang and You attributed this enhancement of heat transfer to an increased number of nucleation sites activated by bubbles departing from lower nucleation sites on the inclined surface. When comparing the 1-cm^2 heater results in Fig. 6 with the 4- and 25-cm^2 heaters in Figs. 7 and 8, however, the effect appears to decrease with increasing surface size. In the higher heat flux range near q''_{CHF}, the 25-cm^2 surface showed a significant difference in heat transfer performance from $\theta = 0°$ to 45° which was not observed in the 1- and 4-cm^2 surfaces in Figs. 6 and 7. This is attributed to an increase in convection heat transfer (similar to flow boiling) caused by the large mass of bubbles departing at an angle from the surface.

The observations in Figs. 6–8 appear to be significantly different to that reported by Nishikawa et al. [5] for boiling water. Marcus and Dropkin [3], Jung et al. [12], Beduz et al. [6], and El-Genk and Guo [7] have all reported results similar to Nishikawa et al.'s. They observed that the surface orientation effect was substantial in the low-heat-flux nucleate boiling region where heat transfer increased as the inclination angle increased from $\theta = 0°$ to 175°. However, Nishikawa et al. have observed this trend below approximately 15% of $q''_{CHF,Z}$ for saturated water. For the present data in Figs. 6–8, this region is dominated by single-phase natural convection under increasing heat flux conditions. Unlike water, FC-72 exhibits a high degree of superheat hysteresis, which means that a higher heat flux is required to initiate nucleation relatively. Due to this significant difference in wall superheat values at incipience between water and FC-72, it would be more appropriate to compare

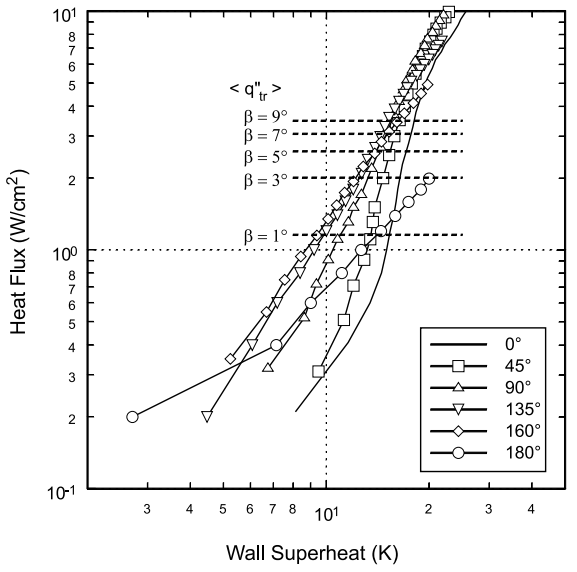

Fig. 9. Effects of inclination angle for 25-cm^2 surface (decreasing heat flux).

decreasing heat flux boiling curves of the present surfaces with those of Nishikawa et al. During the decreasing heat flux boiling curve, the cessation of nucleation occurs at much lower heat-flux values than the incipience.

Nucleate boiling curves of the present plain surfaces in the low-heat-flux region were generated using decreasing heat-flux conditions. For each surface orientation, 80% of the q''_{CHF} value was used as the initial heat-flux point. The test results for the 25-cm^2 surface are presented in Fig. 9. The log-scale is used to provide a better view of the low-heat-flux region. At heat fluxes lower than $\approx$3 W/cm^2, a higher inclination angle provides better nucleate boiling heat transfer except in the 180° case. This trend is consistent with Nishikawa et al.'s observations. Tong et al. [26] have performed a theoretical analysis to quantify the observed orientation effects in low-heat-flux nucleate boiling from the downward-facing inclined surfaces of Nishikawa et al. as well as Githinji and Sabersky [4] and Jung et al. [12]. As isolated bubbles leave the sites, they were thought to sweep along the surface and strip the superheated liquid layer from the heated surface in their paths. The bubble sweeping was considered to enhance the convective heat transfer significantly, and hence a higher heat transfer coefficient was produced by increasing the inclination angle. Comparing the results of the 4-cm^2 surface (not shown) with the results of the 25-cm^2 surface in Fig. 9 shows an additional enhancement with increasing orientation angle when surface size is increased. The bubble sweeping motion along the longer-length 25-cm^2 surface may also maintain a better nucleation mechanism, and thus increase further the nucleate boiling heat transfer over the shorter-length 4-cm^2 surface.

For Nishikawa et al.'s [5] test data for water, the enhancement of nucleate boiling performance from the increased inclination angle disappeared at heat fluxes higher than $\approx$18 W/cm^2. Lienhard [9], using Moissis and Berenson's [11] model, explained this behavior as the transition from the isolated bubble regime to that of slugs and columns. Lienhard explained that bubble frequency and size are controlled by gravity in the isolated bubble regime, and hence surface orientation effects on heat transfer coefficients are significant. The influence of gravity on different orientations appeared to vanish above the transition heat flux. Moissis and Berenson developed an equation to predict the transition heat flux for a flat surface given by

$$q''_{tr} = 0.11 h_{lv} \rho_v^{1/2} [\sigma g/(\rho_l - \rho_v)]^{1/4} \beta^{1/2}. \quad (2)$$

Using Eq. (2), the transitional heat flux is calculated for saturated FC-72. To make this calculation, the fluid-surface contact angle, β, must be known for the FC-72/copper system. Tong et al. [27] have reported that the static contact angle for Fluorinert (FC series by 3M) liquids are very small, approaching zero on polished copper surfaces while the dynamic contact angle could be much larger and was dependent on the interface velocity. The contact angle in Eq. (2) was estimated as 1°, 3°, 5°, 7° and 9° for the q''_{tr} predictions shown in Fig. 9. For the present tests in Fig. 9, the transitional heat flux is observed at $q''_{tr} \approx 3$ W/cm^2 which corresponds to $\beta \approx 7°$. In contrast, Lienhard [9] found that Nishikawa et al.'s [5] data showed $q''_{tr} \approx 18$ W/cm^2 for water, which corresponds to $\beta \approx 60°$.

5.2. Heater orientation effect for microporous surfaces

The boiling curves of the microporous coated surfaces at different inclination angles are shown in Figs. 6–8. The boiling curves were placed on the same graph as the plain surfaces to provide a better comparison. In all microporous coated surface cases, incipient superheats were observed to be less than 12 K – not shown in the figures. The most striking feature of the microporous coated surface results is that the nucleate boiling curves of all angles appear to collapse to one curve. This is due to the higher number of active nucleation sites provided by the microporous structure, which significantly enhances the heat removal mechanism at low heat fluxes, overshadowing any enhancement gained from an increase in inclination angle. For larger surfaces, the microporous boiling data show a pronounced bend in the boiling curve as the heat flux approaches q''_{CHF}.

Fig. 10 shows the data for the 1-, 4-, and 25-cm^2 plain and microporous coated surface boiling curves at all inclination angles. The microporous surface boiling data above the bend (point of maximum heat transfer coefficient) just prior to q''_{CHF} have been omitted for clarity.

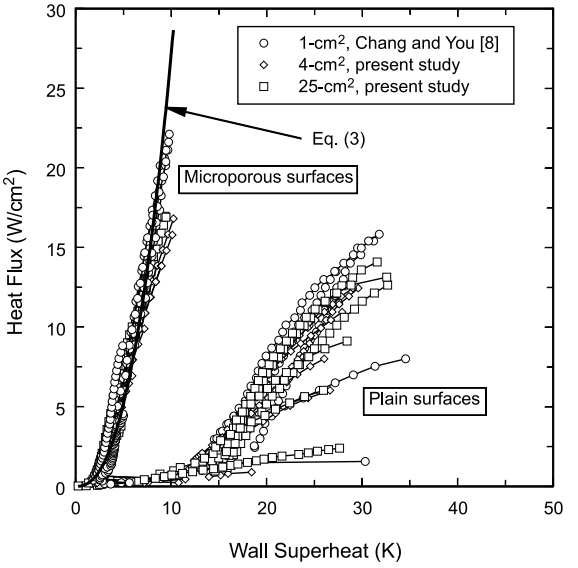

Fig. 10. Effects of size and inclination angle for all surfaces (increasing heat flux).

Although very crowded, this graph helps to illustrate the combined effects of surface size, orientation, and the microporous surface enhancement observed in the data. Interestingly, the observed trends of the effect of heater size on horizontal surface ($\theta = 0°$) nucleate boiling are similar for the plain and microporous coated surfaces – see Fig. 3. For the plain surfaces, surface orientation combined with surface size has been found to affect the boiling performance causing a significant amount of scatter. As shown in Fig. 10, the nucleate boiling data of the microporous coated surfaces for all sizes and inclinations are correlated quite well with a power-law curve fit given by

$$q'' = 1100 \cdot \Delta T_{\text{sat}}^{2.4}. \tag{3}$$

Eq. (3) was obtained by fitting the nucleate boiling curve data of the microporous coated surfaces at all angles and sizes.

5.3. Heater orientation effect on q''_{CHF}

The surface orientation effect on q''_{CHF} is presented in Fig. 11 for the plain and microporous coated surfaces of all surface sizes tested. The q''_{CHF} data were normalized by the q''_{CHF} at $\theta = 0°$. The empirical equation by Chang and You [8] for the 1-cm^2 surface is also plotted in Fig. 11 and is given by

$$\frac{q''_{\text{CHF}}}{q''_{\text{CHF},0°}} = 1.0 - 0.00120 \cdot \theta \cdot \tan(0.414 \cdot \theta) - 0.122 \cdot \sin(0.318 \cdot \theta). \tag{4}$$

The q''_{CHF} values tend to decrease as the inclination angle increases – dramatically decreasing for $135° < \theta < 180°$. As shown in Fig. 11, the present q''_{CHF} data for each surface follow a similar trend with the fitted equation. The similarity in the normalized q''_{CHF} data for each of the different surface conditions confirms that the q''_{CHF} mechanism is a strong function of surface orientation. The 25-cm^2 surfaces showed slight increases in q''_{CHF} at 45° and 90°. As discussed previously in Fig. 8, this is most likely a size effect caused by increased convection heat transfer from bubble sweeping. However, even though this behavior was repeatable, the increase in q''_{CHF} values for the 25-cm^2 surfaces from 0° to 45° and 90° is nearly within experimental uncertainty, therefore, a larger test surface would be required to confirm this observation.

When the surface is near horizontal, the vapor is primarily removed normal to the surface with a correspondingly lower vapor residence time near the surface. The q''_{CHF} mechanism in this case would most likely be dominated by the hydrodynamic aspects as previously modeled by Zuber [1]. As the heater surface is inclined to near vertical, the vapor formed a wavy interface along the surface very much like flow boiling situations. Mudawar et al. [28] have observed for vertical surfaces in FC-72 and water that near q''_{CHF} boiling remained active in the form of wetting fronts and q''_{CHF} occurred when these wetting fronts lifted off the surface. They also developed a model that was identical in form, but not in mechanism, to Zuber's model for horizontal pool boiling. As the inclination angle is further increased to downward-facing angles, the vapor formed large, slower-moving bubbles that were stratified against the surface, significantly increasing the vapor residence time

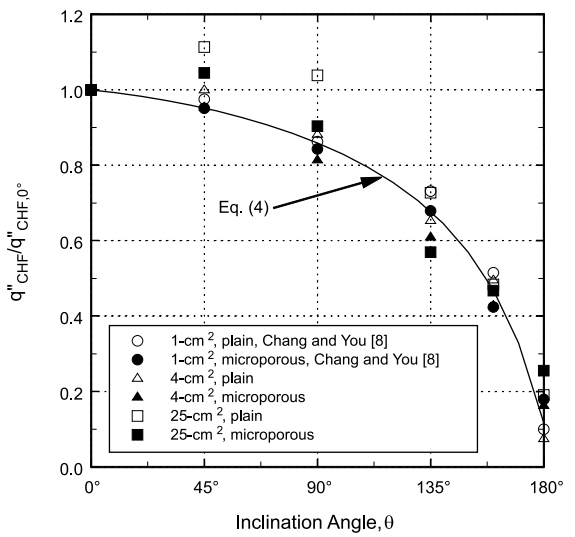

Fig. 11. Normalized CHF data versus inclination angle.

near the surface producing low q''_{CHF} values as previously discussed.

6. Conclusions

To understand the effects of heater orientation and size on the pool boiling performance of plain and microporous coated surfaces, two relatively large, flush-mounted copper surfaces (2 cm × 2 cm and 5 cm × 5cm) were tested and combined with the previous results of Chang and You [8] who studied a 1 cm × 1 cm surface. Two heater surfaces, plain and microporous coated, were tested in saturated FC-72 at atmospheric pressure.

1. The plain surface pool boiling curves showed that the nucleate boiling performance is affected both by the heater orientation and size. The nucleate boiling performance increased slightly from 0° to 45° and then decreased dramatically from 90° to 180°. The dramatic decrease in performance from 90° to 180° is attributed to the significant increase in vapor residence time near the surface of the departing bubbles. In addition, larger surfaces exhibited diminished enhancement from 0° to 45° in the lower heat-flux region, and increased enhancement from 0° to 45° in the higher heat-flux region.
2. Under decreasing heat-flux conditions (below ≈3 W/cm^2), the present heaters showed better heat transfer rates with higher inclination angles up to 135°, similar to Nishikawa et al.'s [5] observations. This increased performance at higher inclination angles is most likely due to continued nucleation from bubbles sweeping along the surface. Above ≈3 W/cm^2, the enhancement effect disappears.
3. Unlike the plain surfaces, the nucleate boiling curves of the microporous enhanced surfaces were insensitive to both inclination angle and heater size due to the higher number of active nucleation sites provided by the surface microstructure. A single empirical correlation, $q'' = 1100 \cdot \Delta T_{sat}^{2.4}$ was shown to predict the microporous coated surface nucleate boiling performance for any surface size or inclination angle in FC-72.
4. The CHF data for all heater sizes and surface conditions tested in the present study showed good agreement with the empirical correlation, Eq. (4), derived previously by Chang and You [8] for FC-72, which confirms that CHF is a strong function of inclination angle. In addition, the CHF mechanism appears to change from "hydrodynamic" to "dry-out" due to the increased vapor residence time near the surface when $\theta > 90°$.
5. The plain and microporous coated surfaces exhibited similar CHF behavior with respect to heater size. For large heaters, the CHF behaved asymptotically while for small heaters, the CHF was higher and showed an inversely proportional relationship with heater size.

Acknowledgements

This study was supported by the Texas Higher Education Coordinating Board: Advanced Research/Technology Program grant number 003656-014. The authors extend their thanks to the 3M Industrial Chemical Products Division for the donation of FC-72 test liquid.

References

[1] N. Zuber, Hydrodynamic aspects of boiling heat transfer, AEC Report No. AECU-4439, Physics and Mathematics, 1959.
[2] A.T. Storr, The effects of heating surface geometry and orientation on nucleate boiling of subcooled water, M.S. Thesis, Washington University, Sever Institute of Technology, Department of Chemical Engineering, 1958.
[3] B.D. Marcus, D. Dropkin, The effect of surface configuration on nucleate boiling heat transfer, Int. J. Heat Mass Transfer 6 (1963) 863–867.
[4] P.M. Githinji, R.H. Sabersky, Some effect of the orientation of the heating surface in nucleate boiling, ASME J. Heat Transfer 85 (1963) 379.
[5] K. Nishikawa, Y. Fujita, S. Uchida, H. Ohta, Effect of surface configuration on nucleate boiling heat transfer, Int. J. Heat Mass Transfer 27 (1984) 1559–1571.
[6] C. Beduz, R.G. Scurlock, A.J. Sousa, Angular dependence of boiling heat transfer mechanisms in liquid nitrogen, Adv. Cryogenic Engrg. 33 (1988) 363–370.
[7] M. El-Genk, Z. Guo, Transient boiling from inclined and downward-facing surfaces in a saturated pool, Int. J. Refrigeration 16 (1993) 414–422.
[8] J.Y. Chang, S.M. You, Heater orientation effects on pool boiling of micro-porous-enhanced surfaces in saturated fc-72, ASME J. Heat Transfer 118 (1996) 937–943.
[9] J.H. Lienhard, On the two regimes of nucleate boiling, ASME J. Heat Transfer 107 (1985) 262–264.
[10] N. Zuber, Nucleate boiling the region of isolated bubbles and similarity with natural convection, Int. J. Heat Mass Transfer 6 (1963) 53–78.
[11] R. Moissis, P.J. Berenson, On the hydrodynamic transition in nucleate boiling, ASME J. Heat Transfer 85 (1963) 221–229.
[12] D.S. Jung, J.E.S. Venart, A.C.M. Sousa, Effects of enhanced surfaces and surface orientation on nucleate and film boiling heat transfer in r-11, Int. J. Heat Mass Transfer 30 (1987) 2627–2639.
[13] D.N. Lyon, Boiling heat transfer and peak nucleate boiling fluxes in saturated liquid helium between the λ and critical temperatures, Adv. Cryogenic Engrg. 10 (1965) 371–379.
[14] I.P. Vishnev, Effect of orienting the hot surface with respect to the gravitational field on the critical nucleate boiling of a liquid, J. Engrg. Phys. 24 (1974) 43–48 (Trans. Inzhenerno-Fizicheskii Zhurnal).

[15] A.H. Howard, I. Mudawar, Orientation effects on pool boiling critical heat flux (chf) and modeling of chf for near-vertical surfaces, Int. J. Heat Mass Transfer 42 (1998) 1665–1688.
[16] I.I. Gogonin, S.S. Kutateladze, Critical heat flux as a function of heater size for a liquid boiling in a large enclosure, J. Engrg. Phys. 33 (1977) 1286–1289 (Trans. Inzhenerno-Fizicheskii Zhurnal).
[17] S. Ishigai, K. Inoue, Z. Kiwaki, T. Inai, Boiling heat transfer from a flat surface facing downward, in: Proceedings of the International Heat Transfer Conference, Boulder, CO, 1961, pp. 224–229.
[18] V.S. Granovskii, A.A. Sulatskii, S.M. Shmelev, The crisis of nucleate boiling on a horizontal surface facing downward, High Temp. 32 (1994) 78–80.
[19] J.H. Lienhard, V.K. Dhir, D.M. Riherd, Peak pool boiling heat-flux measurements on finite horizontal flat plates, ASME J. Heat Transfer 95 (1973) 477–482.
[20] J.R. Saylor, T.W. Simon, A. Bar-Cohen, The effect of a dimensionless length scale on the critical heat flux in saturated, pool boiling, ASME Publication HTD-108 (1989) 71–80.
[21] K.A. Park, A.E. Bergles, Effects of size of simulated microelectronic chips on boiling and critical heat flux, ASME J. Heat Transfer 110 (1988) 728–734.
[22] J.P. O'Connor, S.M. You, D.C. Price, A dielectric surface coating technique to enhance boiling heat transfer from high power microelectronics, IEEE Trans. CPMT, Part A 18 (1995) 656–663.
[23] J.Y. Chang, S.M. You, Boiling heat transfer phenomena from micro-porous and porous surfaces in saturated fc-72, Int. J. Heat Mass Transfer 40 (1997) 4437–4447.
[24] J.Y. Chang, S.M. You, Enhanced boiling heat transfer from micro-porous surfaces: effects of a coating composition and method, Int. J. Heat Mass Transfer 40 (1997) 4449–4460.
[25] A. Bar-Cohen, A. McNeil, Parametric effects of pool boiling critical heat flux in dielectric liquids, ASME Pool and External Flow Boiling (1992) 171–175.
[26] W. Tong, A. Bar-Cohen, T.W. Simon, A bubble sweeping heat transfer mechanism for low flux boiling on downward-facing inclined surfaces, ASME Publication HTD-104 (1988) 173–178.
[27] W. Tong, A. Bar-Cohen, T.W. Simon, S.M. You, Contact angle effects on boiling incipience of highly-wetting liquids, Int. J. Heat Mass Transfer 33 (1990) 91–103.
[28] I. Mudawar, A.H. Howard, C.O. Gersey, An analytical model for near-saturated pool boiling critical heat flux on vertical surfaces, Int. J. Heat Mass Transfer 40 (1997) 2327–2339.